Curvature Effects on Film Cooling with Injection Through Two Rows of Holes

K. Jung, D.K. Hennecke
Darmstadt University of Technology
Gas Turbines and Flight Propulsion
Petersenstr. 30, 64287 Darmstadt, Germany

Abstract

The adiabatic film cooling effectiveness on convex and concave curved surfaces (as a model for suction and pressure side film cooling of gas turbine blades) with two staggered rows of injection holes are investigated by using a mass transfer technique. Additionally measurements on a flat plate are made for comparison. Two different radii of curvature (R/D = ±60, ±120) and two streamwise distances of the rows (12D and 24D) with film cooling holes inclined at 40° are considered. The blowing rates are varied in a wide range from 0.25 to 2.0 and the main stream Reynolds numbers (Re_D) between 10000 and 50000. At low and moderate blowing rates the effectiveness is enhanced on convex and reduced on concave curved surfaces compared to results obtained on the flat surface. At high blowing rates the effectiveness is not greatly influenced by surface curvature. The effect of curvature was found to be negligible between the two rows and reduced downstream of the second row compared to results described in the literature for single row injection.

Introduction

An improvement of thermal efficiency of modern gas turbines is achieved by increasing compressor pressure ratios and turbine inlet temperatures. This temperature increase demands highly sophisticated cooling techniques to ensure a reasonable lifetime of the thermally exposed components. Today turbine blades are commonly cooled by a combination of internal convection and impingement cooling and external film cooling. The tasks in design hereby are to achieve an optimum cooling by a minimum of cooling air and to minimize the aerodynamic losses which are an unwanted consequence of the film cooling measures. In today's design methods the thermal effects of the cooling film are still taken into account by use of simple correlations. It must be kept in mind, that an under-prediction of the blade-surface temperature of only 15K may reduce the lifetime up to 50%.

Over the past 40 years, film cooling has been the subject of many investigations. Most of these studies concentrate on flat plate geometries with injection through slots or rows of cylindrical holes. A detailed survey of flat plate film cooling research up to 1971 has been provided by Goldstein [8]. Other publications are available dealing with leading edge geometries, simplified pressure or suction side geometries or specific airfoil geometries. Results of theses studies show that surface curvature can significantly modify film cooling performance. The first investigations focusing on the influence of curvature have been published by Nicolas and Le Meur [18], Folayan and Whitelaw [4] and Mayle et al. [17]. They conducted measurements on generic curved walls with slot injection. Compared to the results on flat surfaces, injection at low blowing rates (M = 0.5) increases adiabatic film cooling effectiveness on convex and decreases it on concave curved surfaces. For moderate blowing rates (M = 1.0), the film cooling effectiveness is higher on convex than on flat and concave surfaces. In contrast to the results for low blowing rates, high blowing rates (M = 2.0) enhances the adiabatic wall effectiveness on concave curved surfaces compared to flat and convex surfaces. Generally, the effect of

Paper presented at the RTO AVT Symposium on "Advanced Flow Management: Part B – Heat Transfer and Cooling in Propulsion and Power Systems", held in Loen, Norway, 7-11 May 2001, and published in RTO-MP-069(I).

Report Documentation Page			*Form Approved* *OMB No. 0704-0188*
Public reporting burden for the collection of information is estimated to average 1 hour per response, including the time for reviewing instructions, searching existing data sources, gathering and maintaining the data needed, and completing and reviewing the collection of information. Send comments regarding this burden estimate or any other aspect of this collection of information, including suggestions for reducing this burden, to Washington Headquarters Services, Directorate for Information Operations and Reports, 1215 Jefferson Davis Highway, Suite 1204, Arlington VA 22202-4302. Respondents should be aware that notwithstanding any other provision of law, no person shall be subject to a penalty for failing to comply with a collection of information if it does not display a currently valid OMB control number.			
1. REPORT DATE **00 MAR 2003**	2. REPORT TYPE **N/A**		3. DATES COVERED **-**
4. TITLE AND SUBTITLE **Curvature Effects on Film Cooling With Injection Through Two Rows of Holes**			5a. CONTRACT NUMBER
			5b. GRANT NUMBER
			5c. PROGRAM ELEMENT NUMBER
6. AUTHOR(S)			5d. PROJECT NUMBER
			5e. TASK NUMBER
			5f. WORK UNIT NUMBER
7. PERFORMING ORGANIZATION NAME(S) AND ADDRESS(ES) **NATO Research and Technology Organisation BP 25, 7 Rue Ancelle, F-92201 Neuilly-Sue-Seine Cedex, France**			8. PERFORMING ORGANIZATION REPORT NUMBER
9. SPONSORING/MONITORING AGENCY NAME(S) AND ADDRESS(ES)			10. SPONSOR/MONITOR'S ACRONYM(S)
			11. SPONSOR/MONITOR'S REPORT NUMBER(S)
12. DISTRIBUTION/AVAILABILITY STATEMENT **Approved for public release, distribution unlimited**			
13. SUPPLEMENTARY NOTES **Also see ADM001490, presented at RTO Applied Vehicle Technology Panel (AVT) Symposium held in Leon, Norway on 7-11 May 2001, The original document contains color images.**			
14. ABSTRACT			
15. SUBJECT TERMS			

16. SECURITY CLASSIFICATION OF:			17. LIMITATION OF ABSTRACT	18. NUMBER OF PAGES	19a. NAME OF RESPONSIBLE PERSON
a. REPORT **unclassified**	b. ABSTRACT **unclassified**	c. THIS PAGE **unclassified**	**UU**	**14**	

Nomenclature

c	mass concentration
c_p	pressure coefficient
D	cooling hole diameter
gv	gray value
h	heat transfer coefficient
I	momentum flux ratio, $\left(\rho_2 u_2^2\right) / \left(\rho_\infty u_\infty^2\right)$
L	length of cooling hole
M	blowing rate, $\left(\rho_2 u_2\right) / \left(\rho_\infty u_\infty\right)$
p	pressure
P	pitch, lateral spacing of film holes
$\dot{q}$	heat flux
R	radius of (surface) curvature
Re	Reynolds number
S	streamwise spacing of rows
T	temperature
u	velocity
x	streamwise coordinate
x^*	x downstream of 2nd row
y	coordinate normal to x and z
z	lateral/spanwise coordinate
Greek symbols	
δ_1	displacement thickness
γ	injection angle
η	film cooling effectiveness
ρ	density
Subscripts	
aw	adiabatic wall
iw	impermeable wall
p	potential
s	static
t	total
0	without film cooling
2	injection
∞	mainstream

curvature seems to be more pronounced on the (convex) suction side. In addition to the measurements of the film cooling effectiveness, Mayle et al. [17] presented boundary-layer velocity and temperature measurements. They attributed the effects described above to "… the effect curvature has on the production, diffusion and dissipation of Reynolds stresses and the turbulent heat flux".

Most of the studies concerned with curvature effects on film cooling performance were conducted with injection through a single row of cylindrical holes. Ito et al. [10] compared airfoil pressure and suction side effectiveness with flat plate data, and developed an analytical criterion for favorable coolant momentum fluxes as function of the surface curvature. Kruse [12], Schwarz and Goldstein [20] and Schwarz et al. [21] presented results for generic curved surfaces (convex , concave and flat plate) with variation of the surface curvature to cooling hole diameter ratio. The laterally averaged film cooling effectiveness was observed to increase with increasing curvature (-1/R to +1/R) especially for small blowing rates until the coolant film separates on a strongly curved wall. Schwarz et al. [21] pointed out, that lateral profiles of local effectiveness are much flatter on the concave surface than on the convex one. This is attributed to lateral mixing caused by unstable concave flow. It results – especially for higher blowing rates – in blockage between the coolant jets and therefore in a slotlike behavior for row of holes injection. Lutum et al. [14], [15] investigated the influence of the streamwise pressure gradient, $\partial p/\partial x$, on film cooling performance on a convex curved surface. The effect of streamwise pressure gradient seems to be more pronounced on a curved surface than for flat plate film cooling.

Film injection through two or more rows of holes have a favorable influence on film cooling performance as experiments on flat plate configurations showed (e.g. Jabbari and Goldstein [11], Martinez-Botas and Yuen [16]). Depending on the configuration used it is possible to reach a slotlike behavior. In spite of the importance and the engine-like geometry of such configurations, only few investigations dealing with film injection through two or more rows of holes are published. Lander et al. [13] performed measurements on a turbine airfoil in a linear cascade with film injection through two staggered rows. Drost and Bölcs studied heat transfer and film cooling effectiveness on a turbine airfoil with single row injection on the pressure side (PS) and single or double row injection on suction side (SS). Comparisons of these two cooling configurations on the SS revealed a better film cooling performance of the double row due to an improved film coverage and delay jet separation. Goldstein et al. [7] investigated film cooling on convex and concave curved surfaces for double row injection. The results were compared to measurements on curved surfaces with single row injection and to flat plate experiments. Surface curvature affected film cooling performance with injection through one or two rows of staggered holes significantly. The influence of curvature, however, was less than with injection through a single row of holes. Goldstein et al. [7] attributed this effect to the fact, that jets from a single row tend to act more independently.

Experimental Facility and Procedure

Measurement Technique

As shown by several authors (e.g. Eckert [2], Goldstein [8]) the effects of film cooling can be described by separating them into a hydrodynamic effect quantified by the heat transfer coefficient with film cooling

$$h_f = \frac{\dot{q}}{T_w - T_{ad}} \tag{1}$$

and a thermodynamic effect quantified by the adiabatic film cooling effectiveness (the dimensionless adiabatic wall temperature):

$$\eta_{aw} = \frac{T_{aw} - T_\infty}{T_2 - T_\infty}. \tag{2}$$

The present measurements of the adiabatic film cooling effectiveness have been conducted using the "Ammonia and Diazo Technique With CO_2-Calibration" described in detail by Haslinger and Hennecke [9]. Based on the analogy between heat an mass transfer the adiabatic film cooling effectiveness can be described by the dimensionless concentration of a tracer gas along the impermeable wall:

$$\eta_{aw} = \frac{c_{iw} - c_\infty}{c_2 - c_\infty}. \tag{3}$$

The measurement technique consists of two separate parts. In the ammonia and diazo part of the experiment a diazo film is mounted on the model surface and a mixture of ammonia (NH_3) and air ($c_2 \approx 1 \ldots 2\%$) is blown out of the cooling holes. Depending on the wall concentrations of the ammonia the diazo film reacts building a distribution of gray color. This is digitized using a scanner and results in a highly resolved distribution (150*dpi*) of gray values $gv(x, z)$. In the calibration part of the experiment carbon dioxide (CO_2) instead of ammonia is used as a tracer gas ($c_2 \approx 2\%$). Gas samples are sucked off and analyzed at some locations (x_i, z_i) along the wall giving local values of adiabatic effectiveness $\eta_{ad}(x_i, z_i)$ from Eq. (3). From $\eta_{ad}(x_i, z_i)$ and the gray values $gv(x_i, z_i)$ at the same positions a calibration function $\eta_{ad} = f(gv)$ is calculated. This is applied to the *gv*-distribution resulting in a highly resolved distribution of the adiabatic film cooling effectiveness.

Test Facility

The measurements were conducted in an open circuit subsonic wind tunnel (see Fig. 1). The air passes an inlet plenum with screens and flow straighteners, a nozzle with a contraction of 10.7:1, a 570*mm* long duct, the test section (see Fig. 2), a diffusor and finally an axial blower. The test section with a 145 (radial) by 826*mm* (lateral) cross-section was optimized using a commercial CFD-code (CFX-Tascflow) to reduce secondary flow of the first kind and in order to prevent flow separation. Depending on the key test parameters listed in Table 1, the mainstream velocity varies between 15 *m/s* and 75 *m/s*. Two 1.0-*mm*-tripwires were positioned in the straight duct between nozzle and test section to produce turbulent boundary layers at all mainstream velocities.

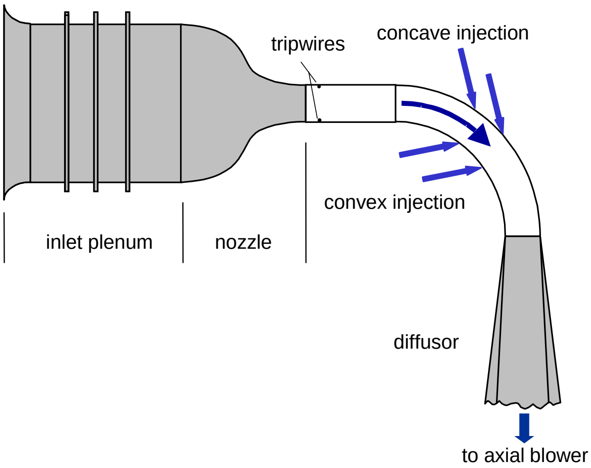

Fig. 1: Experimental facility - schematic

Test section and cooling geometry

The complete test section is made exchangeable to allow variation of curvature radius. All test surfaces (convex and concave) have the same length resulting in a 90° curve for *R/D* = ±60 and a 45° curve for R/D = ±120. The material of the injection wall is aluminum to ensure a uniform temperature distribution. The top and bottom plate and the second (non-injection) wall are made of plexiglass. The coolant flow is injected through two staggered rows of eight holes that are 10mm in diameter with 4*D* lateral spacing, 12D or 24D streamwise spacing and a streamwise injection angle γ of 40° (see Table 1 and Fig. 2). The first row is located 30*D* from onset of curvature. Small taps that are 0.6*mm* in diameter are located along the injection wall downstream on the centerlines of one injection hole of the first and one of the second row. These taps are used for static pressure measurements and to sampling gas for the calibration experiment.

Secondary Flow and Gas Sampling

The secondary flow system is schematically shown in Fig. 3. The air is delivered by a radial blower. In the mixing chamber it is mixed with the tracer gas. The ammonia is taken from a gas cylinder of liquid ammonia, is led through a pressure regulator and a (calibrated) fine needle valve and is then mixed with the air in the mixing chamber. In the calibration experiment with CO_2, the gas is provided in the same way. Then the mixture is split to ensure that the blowing rate of each row can be adjusted separately. Both cooling mass flows are regulated by use of a mass flow meter and a controlling valve. In order to get a nearly uniform blowing rate over all cooling holes, the two plenum chambers are fed through one tube in the top and one in the bottom plate. Inside the plenum additional screens were positioned.

Table 1: Key test parameters

GEOMETRICAL	***R/D***	∞, +60, +120, -60, -120[1]
	P/D	4
	S/D	12, 24
	L/D	5
	γ	40°
FLOW CONDITIONS	$\mathbf{Re_D}$	10,000 … 50,000
	M	0.25 … 2.0
	ρ_2/ρ_∞	≈ 1.0

[1] Positive values mean convex, negative values concave curvature.

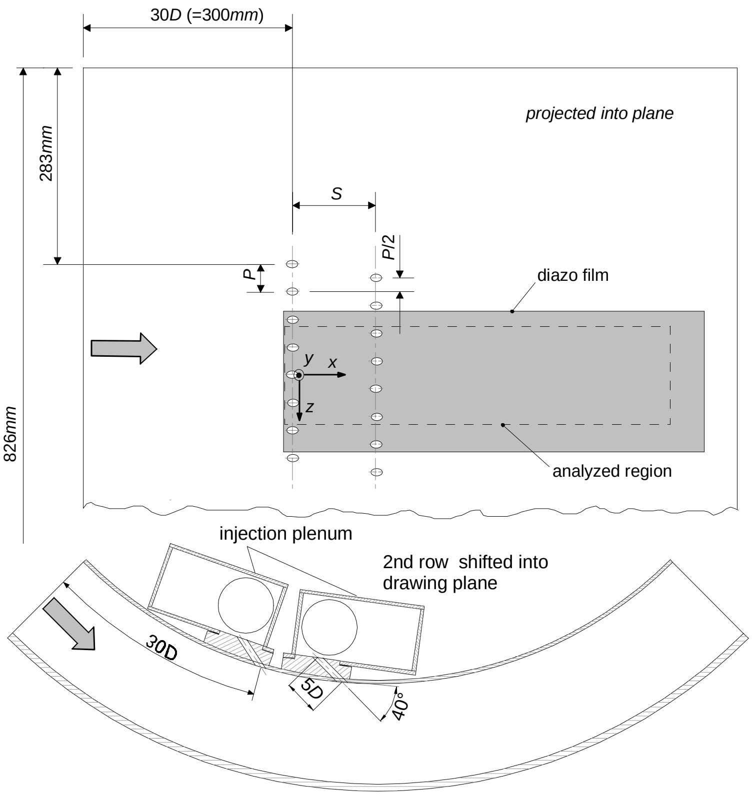

Fig. 2: Schematic view of test section (R/D = +60, S/D = 12)

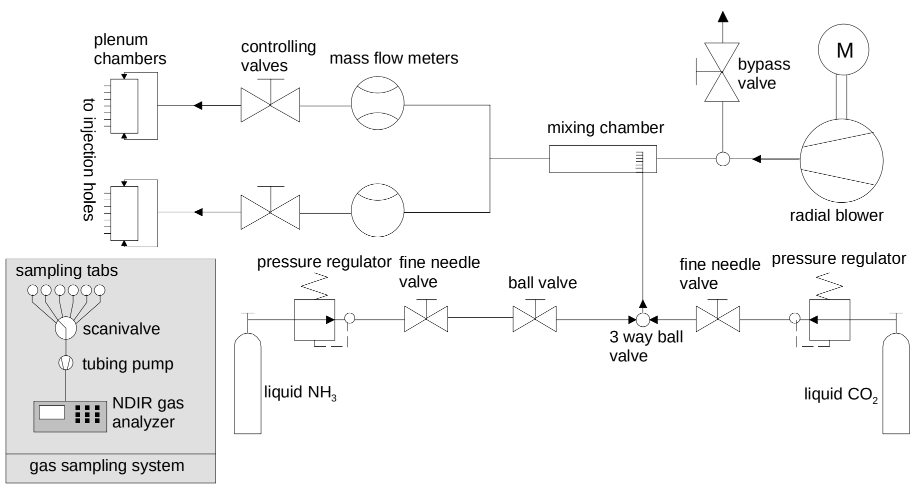

Fig. 3: Secondary flow system

The gas samples are sucked off by a tubing pump connected to a scanivalve that switches between the sampling taps in the test section and two probes located in one plenum chamber and the mainstream flow. The samples are analyzed by an NDIR-analyzer. Following the suggestions of Pedersen [19] suction velocities are less than 2% of the mainstream velocity in order to measure the real wall concentration.

Test conditions

On the basis of the geometrical test parameters listed in Table 1, ten different injection geometries were examined whose notations are listed in Table 2.

Table 2: Notation of test models

	models									
	A	**B**	**C**	**D**	**E**	**F**	**G**	**H**	**I**	**J**
R/D	∞	∞	+120	+120	+60	+60	-120	-120	-60	-60
S/D	12	24	12	24	12	24	12	24	12	24

Due to the high traction ratio of the nozzle between plenum and test section main stream turbulence is very low and was measured to be less than 0.5% for all relevant velocities. As listed in Table 1 tests were conducted for Re_D = 10000, 30000, 40000 and 50000. Blowing rates were varied between 0.25 and 2.0. The blowing rate

$$M = \frac{\rho_2 u_2}{\rho_\infty u_p} \tag{4}$$

is defined using the local (theoretical) potential velocity u_p at the edge of the boundary layer:

$$\frac{u_p}{u_\infty} = \sqrt{1 - c_p}\ . \tag{5}$$

u_p is determined from measurements of static wall pressure (see section "*Flow Measurements*") expressed as the pressure coefficient c_p:

$$c_p = \frac{p_{s,w} - p_{s,\infty}}{0.5 \rho_\infty u_\infty^2} \tag{6}$$

As described in detail by Haslinger and Hennecke [9] the absolute uncertainty of the ammonia and diazo experiment regarding the adiabatic film cooling effectiveness is estimated to be less than 0.05.

Results and discussion

<u>*Flow Measurements*</u>

Aerodynamic measurements of the velocity profiles without secondary air injection were conducted to characterize the freestream flow in the test section. Fig. 4 shows the distribution of the pressure coefficient c_p along the centerline of one blowing hole of the first row (z/D = 0) for different curvature radii. One would expect that the pressure coefficient is 0 at the beginning of curvature. But due to the fact that the static pressure of the undisturbed mainflow $p_{s,\infty}$ is measured directly behind the nozzle and not at the beginning of the test section, there are some differences caused by the pressure losses in the

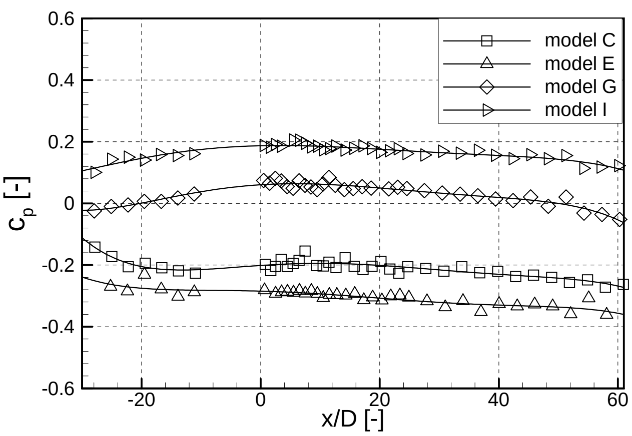

Fig. 4: Pressure coefficient for different curvature radii (Re_D = 30000)

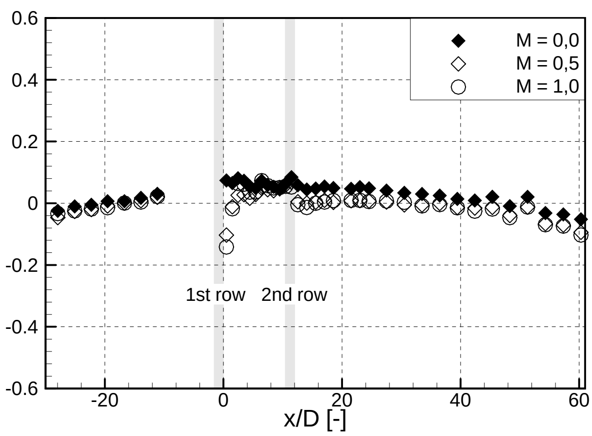

Fig. 5: Pressure coefficient with injection (model G, Re_D = 30000)

straight duct between nozzle and test section. The distribution of the pressure coefficient for the different test models shows the influence of curvature. The centrifugal force caused by streamline curvature enhances the static pressure on concave walls (models G and I) and reduces the pressure on convex walls (models C and E). Due to higher centrifugal forces for stronger curvature this effect is more pronounced for the curvature radius *R/D* = +60 and *R/D* = -60, respectively. Between onset of curvature and the first row of cooling holes (*x/D* = -30.7 … 0) there is a favorable pressure gradient on the convex surfaces and an adverse pressure gradient on the concave walls. The distribution of the pressure coefficient shown in Fig. 4 indicates a nearly zero pressure gradient flow within the relevant part (*x/D* = 0 … 50) of all test sections. Fig. 5 shows the influence of film injection on the pressure coefficient. Compared to the case of no injection (*M* = 0) the static wall pressure immediately downstream of the hole is decreased probably because of separation of the jet from the wall. This effect is a bit more pronounced for higher blowing rates. Only a small effect can be seen downstream of the second row because in this area, the pressure taps are located between two holes. Farther downstream the influence of the cooling jets on the c_p-values is very small.

Fig. 6 compares the normalized streamwise velocity upstream of the test section for different test models (i.e. curvature radii). The measurements were accomplished with a gooseneck pitot probe. The results indicate that there is no recognizable effect of curvature on velocity distribution upstream of the onset of curvature. The distributions of the normalized velocity are in good agreement with the theoretical 1/7-boundary-layer-profile. Fig. 7 shows the distribution of the normalized streamwise velocity directly upstream of the first row (*x/D* = –2) for a curvature radius of R/D = +60 (configuration E, F)[2]. Due to the acceleration on the convex wall the boundary layer thickness is decreased on the convex surface compared to the distribution received with configuration A (flat plate) at the same position. Because of the decelerating free stream flow on the concave surface the boundary layer thickness on this wall is increased.

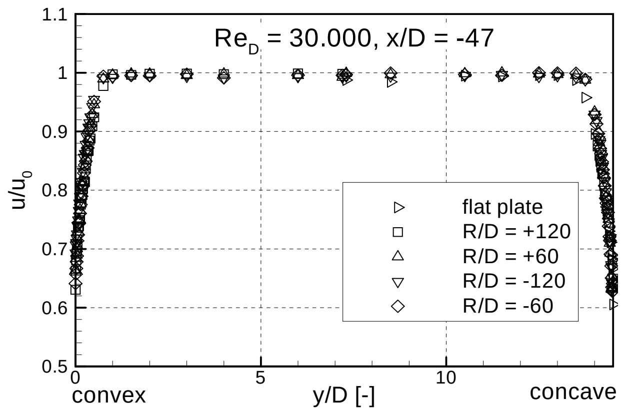

Fig. 6: Normalized streamwise velocity upstream of test section (x/D = -47)

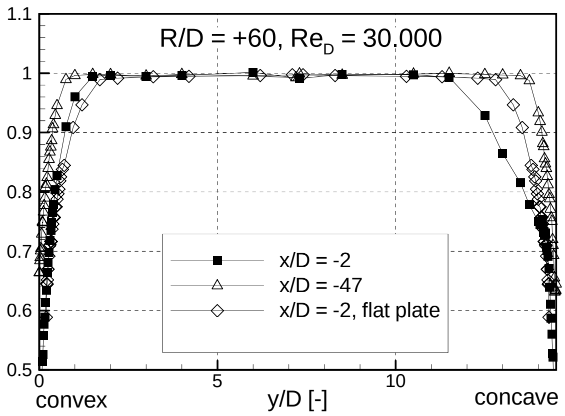

Fig. 7: Normalized streamwise velocity upstream of the first row (x/D = -2)

<u>*Adiabatic Effectiveness*</u>

Fig. 8 compares film cooling effectiveness values obtained on model A and model B (flat plate) for different blowing rates. For low blowing rates (*M* = 0.25 … 0.5) the jets are kept close to the wall resulting in high values of the laterally averaged film cooling effectiveness near the injection. Farther downstream the effectiveness is monotonously decreasing due to mixing with the main stream resulting in coolant dilution. For the lowest blowing rate (*M* = 0.25) this effect is highly pronounced be-

[2] In this case the velocity distribution is normalized with the theoretical potential velocity in a curved duct. All other velocities are normalized using the velocity of the undisturbed mainflow.

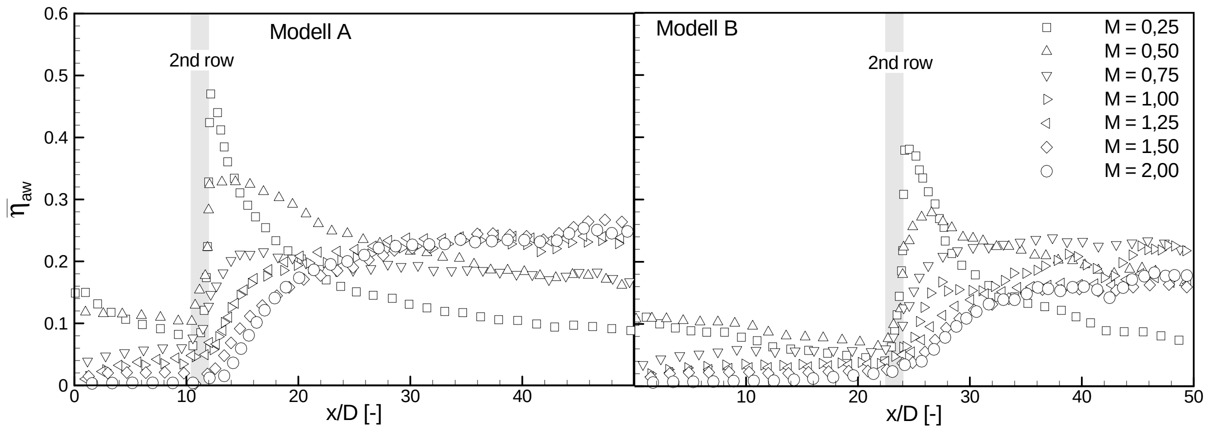

Fig. 8: Distributions of the laterally averaged adiabatic film cooling effectiveness values versus streamwise distance. Comparison of different row spacings (Re_D = 10000, left: S/D = 12, right: S/D = 24).

cause of the very low injected coolant mass flow. For higher blowing rates the jets lift off the surface immediately after injection resulting in low values of laterally averaged effectiveness in this region. Moving downstream the film cooling effectiveness increases monotonously. This is due to jet reattachment and the greater coolant mass introduced into the boundary layer in this area. The effects described above can be found downstream of both rows, but they are more pronounced behind the second row where the level of effectiveness is substantially higher. This is due to lower penetration of jets of the second row because of their interactions with the jets of the first row. Especially for higher blowing rates (i.e. higher amount of coolant) the gaps between the jets of the second row are filled in by jets of the other row promoting blockage. This results in a more slotlike behavior of the cooling film downstream of the second row. For high blowing rates (M = 1.5, 2.0) the jets do not seem to reattach to wall between the two rows. Comparison of the two different row spacings shows that the laterally averaged film cooling effectiveness values downstream of the second row are more increased for S/D = 12 than for S/D = 24 (for the same streamwise distance downstream of the 2nd row). This is due to the enhanced interaction of the jets from the first and the second row for this configuration. Additionally the approaching boundary layer is thicker at x/D = 24 resulting in a reduced effectiveness at this point of injection. This latter effect is attributed to deeper jet penetration (e.g. by Eriksen and Goldstein [3]) or to enhanced lateral mixing (e.g. Foster and Lampard [5]).

Fig. 9 compares distributions of the laterally averaged film cooling effectiveness values for different convex curvatures and different blowing rates. There is only a negligible influence of curvature between the two rows. Downstream of the second row increasing curvature results in enhanced values of the film cooling effectiveness at low and moderate blowing rates ($M \approx 0.25 \dots 1.0$). Increasing the

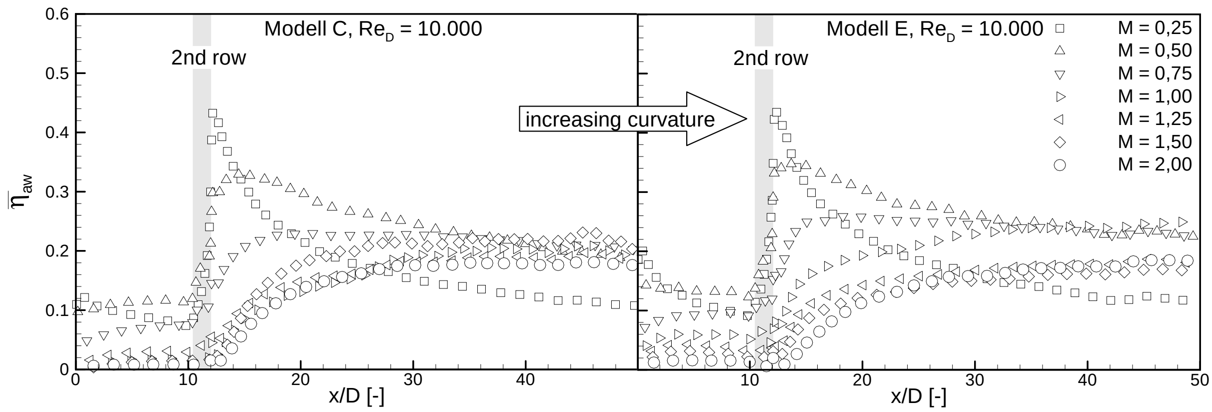

Fig. 9: Distributions of the laterally averaged adiabatic film cooling effectiveness values for two different convex curvatures (S/*D* = 12, Re_D = 10000; left side: *R/D* = +120, right side: *R/D* = +60)

blowing rate beyond M = 1.25 results in an opposite behavior. In this case increasing curvature decreases slightly the laterally averaged film cooling effectiveness. Similar trends for single row injection are found by several authors (e.g. Kruse [12], Schwarz et al. [21]). The effects described above are caused by the cross-stream pressure gradient whose strength is determined by the main flow geometry (i.e. the curvature radius) and the tangential momentum of the jets ($I\cos^2\gamma$). The pressure gradient works to push a film cooling jet into a convex curved wall. The centrifugal force of the jet is determined by its tangential momentum and trends to pull it off a convex wall. At low blowing rates the cross-stream pressure gradient overbalances the centrifugal force of the jet and therefore the jets are pushed into the wall. Beyond an optimum blowing rate, where the centrifugal force and the pressure gradient are balanced, the centrifugal force overbalances the cross-stream pressure gradient and therefore the jets are pulled off the convex wall.

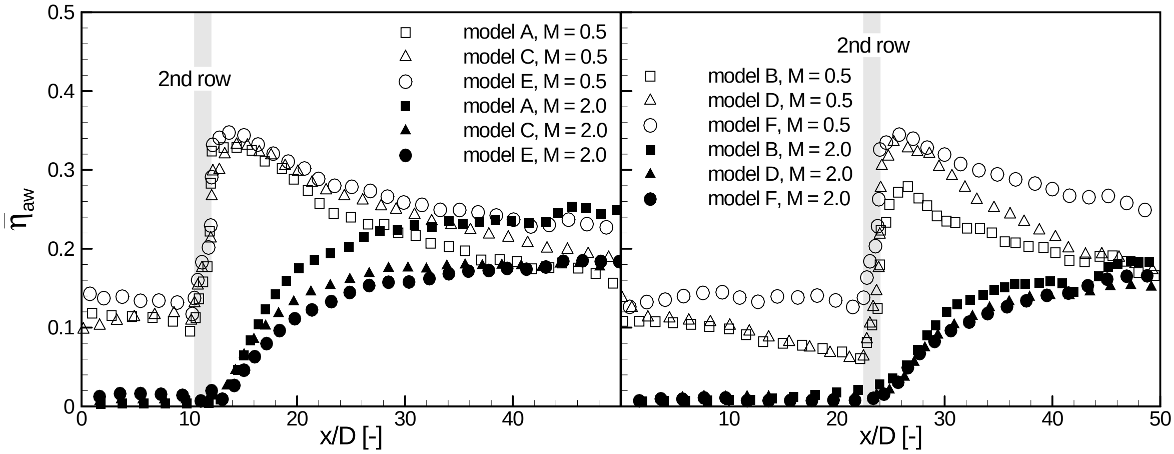

Fig. 10: Distributions of laterally averaged adiabatic film cooling effectiveness values on convex and flat surfaces with different row spacings (Re_D = 10000; left side: *S/D* = 12, right side: *S/D* = 24)

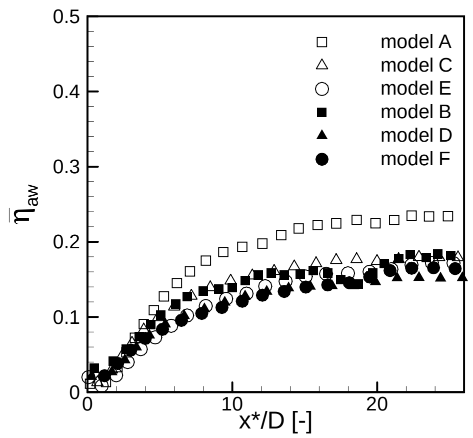

Fig. 11: Laterally av. effectiveness downstream of second row (*M* = 2.0)

Fig. 10 compares the effect of different row spacings on the laterally averaged effectiveness obtained on convex and flat surfaces. At a low blowing rate of M = 0.5 both injection configurations show the same behavior: increasing curvature increases the adiabatic effectiveness. As mentioned above this effect is more pronounced downstream of the second row. At a high blowing rate of M = 2.0 increasing curvature (from *R/D* = +120 to *R/D* = +60) results in a negligible decrease of the laterally averaged film cooling effectiveness. The configurations with 12*D* row spacing show (at M = 2.0) an obvious difference between the results obtained on the flat wall compared to the results of the convex curved walls, whereas the differences for the configurations with 24*D* row spacing are very small[3]. Comparisons of the distributions downstream of the second row (Fig. 11) show only small differences between the results obtained on the curved walls (models C, E, D, F) whereas the influence of row spacing is substantially more pronounced on the flat wall. This could refer to the

[3] This behavior refers to the region downstream of the second row, the laterally averaged adiabatic effectiveness values between the two rows are to small to determine a recognizable influence.

fact that the influence of surface curvature on film cooling effectiveness with injection through two rows of holes is less than that with injection through a single row of holes where the jets tend to act more independently as Goldstein et al. [7] pointed out. In this case the differences between the two base configurations (*S/D* = 12 and 24) are mainly caused by the differences in boundary layer thickness at *x/D* = 12 and *x/D* = 24. The growth in boundary layer thickness between *x/D* = 12 and 24 is greater on the flat wall than on the convex curved surfaces due to the accelerated mainstream for this latter geometry. In this case the differences in penetration of the jets of the second row for the two base configurations are probably smaller with injection on convex curved surfaces than with injection on flat walls. Thus the influence of row spacing on the distributions of the laterally averaged film cooling effectiveness is reduced on convex curved surfaces.

In Fig. 12 comparisons of the results for flat, convex and concave walls are shown at Re_D = 10000 and *S/D* = 12 and S/*D* = 24 respectively. Between the two rows no recognizable influence of curvature can be found probably due to the interaction of the jets of the first and the second row. Possibly the jets of the first row are guided by the jets of the second row due to the interaction of the counter-rotating kidney vortices. This behavior could revoke the effect of curvature. The results downstream of the second row are in reasonable agreement with results of several studies conducted with injection through a single row of cylindrical holes (e.g. Ito et al. [10], Kruse [12], Schwarz et al.[21]): At low blowing rates (*M* = 0.5) the laterally averaged adiabatic film cooling effectiveness for both injection configurations is increased on convex and decreased on concave curved surfaces compared to the results obtained on the flat wall. This is because the effects of cross-stream pressure gradient greatly overshadow the effects of the normal and tangential momentum of the jet. At high blowing rates (*M* = 2.0) the laterally averaged adiabatic film cooling effectiveness is decreased on convex curved surfaces (more pronounced for small row spacings as described above) and slightly increased on concave curved surfaces compared to the results obtained on the flat wall. This behavior is due to the tangential momentum of the jet (and therefore the centrifugal force) overbalancing the cross-stream pressure gradient, thereby pushing the jets into the concave wall and pulling it away from the convex wall. As Schwarz et al. [21] pointed out, lateral profiles of local effectiveness are much flatter on the concave surface than on the convex due to enhanced lateral mixing caused by unstable concave flow. This leads to an increased coolant dilution and therefore to a decrease in the adiabatic film cooling effectiveness. The enhanced lateral mixing additionally results – especially for higher blowing rates – in blockage between the coolant jets and therefore in a slotlike behavior. Due to these facts, the influence of concave curvature at high blowing rates is less pronounced compared to convex curvature.

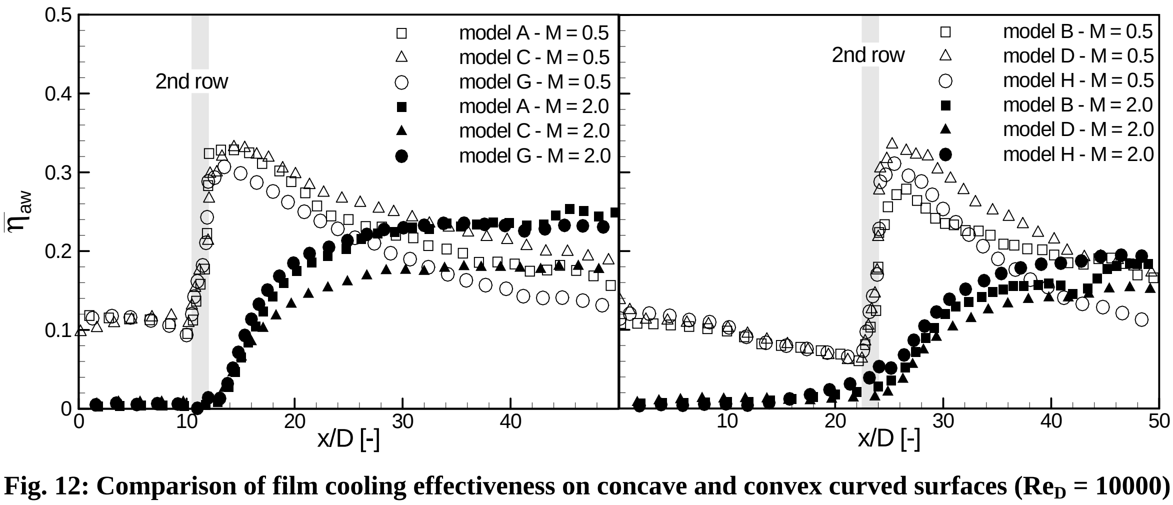

Fig. 12: Comparison of film cooling effectiveness on concave and convex curved surfaces (Re_D = 10000)

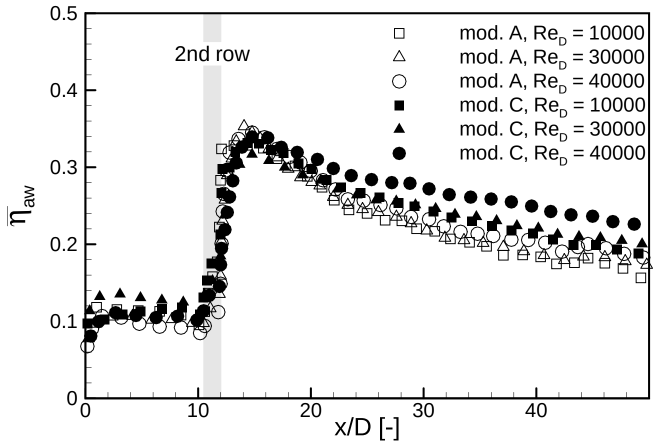

Fig. 13: Influence of Reynolds number

The laterally averaged adiabatic film cooling effectiveness results shown in Fig. 13 for film injection on a flat wall and a convex curved surface (model C) indicate a slightly increased influence of the Reynolds number on curved surfaces. Analogous to the results presented above, this effect is a bit more pronounced downstream of the second row. But the differences in the effectiveness values are in the order of magnitude of the uncertainty of the measurement technique used. Generally the influence of the Reynolds number on the laterally averaged film cooling effectiveness is attributed to stronger jet deflection and a slightly stronger spreading of the jet with increasing Reynolds number.

In Fig. 14, highly resolved distributions of the adiabatic film cooling effectiveness for convex, flat and concave walls are presented at M = 0.50 and M = 2.0 respectively. At low blowing rates, only negligible differences between the two rows can be found as mentioned above for the laterally averaged effectiveness results. Downstream of the second row the lateral effectiveness profiles seem to be steeper on the convex and flatter on the concave than on the flat surface. This can be attributed to the influence the cross-stream pressure gradient has on the structure of the jets, as discussed by Schwarz et al. [21] and Ito et al. [10]. The cross-stream pressure gradient produces flow instabilities on the concave surface which enhances lateral mixing and flattens the jet. On the convex surface the cross-stream pressure gradient suppresses mixing in the convex-wall boundary layer. Therefore, the jets seem to remain distinct much farther downstream on the convex wall. This effect is also described by Goldstein and Stone [6]. Due to the reduced mixing with the mainstream downstream of the second row (see above), these effects are less pronounced than for single row injection.

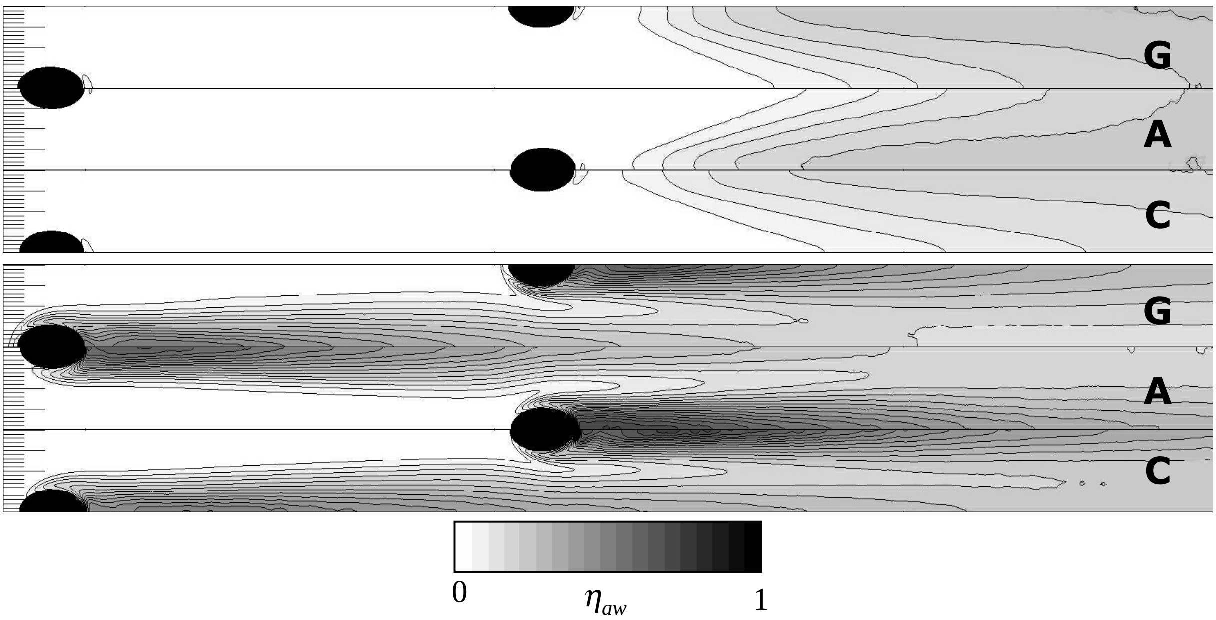

Fig. 14: Distributions of the η_{aw} (Re_D = 10000, lower fig.: M = 0.5, upper fig.: M = 2.0)

At high blowing rates, the surface between the two rows seems to be nearly uncooled due to jet lift-off. The contour plots indicate lower effectiveness values on the convex than on the flat surface. This is due to the deeper jet penetration for this former configuration (at high blowing rates). The contour lines for the concave configuration are similar to the contour lines for the flat configuration, only the profiles seems to be a bit more flattened. The jets of the first row do not reattach to the wall for all three configurations.

Conclusions

In the present study the adiabatic film cooling effectiveness on flat as well as convex and concave curved test surfaces (as a model for suction and pressure side film cooling) with two staggered rows of injection holes was investigated. The radius of curvature, the row spacing, the blowing rate and the mainstream Reynolds number were varied.

- Detailed measurements of the adiabatic film cooling effectiveness have been presented.
- Injection through two staggered rows of holes provided superior film cooling effectiveness downstream of the second row. The lateral profiles in this region seem to be more balanced than for single row injection. The enhanced effectiveness values downstream of the second row are due to the interaction of the jets of both rows.
- The influence of curvature seems to be less with injection through two staggered rows of holes than with injection through a single row of holes. Between the two rows, the influence of curvature was found to be very small for most of the test cases. Downstream of the second row the effects are more pronounced.
- The adiabatic film effectiveness is higher on the convex surface than on a flat or concave surface at low and moderate blowing rates. For higher blowing rates, this trend reverses. But the effects at high blowing rates seems to be less pronounced than at low blowing rates. This can be attributed to the enhanced jet interaction of the jets resulting in a slotlike behavior (and therefore a reduced mixing with the mainstream) downstream of the second row.
- The effect of row spacing is more pronounced on flat surfaces than on curved surfaces due to reduced boundary layer growth between the two rows for the latter configuration.

Acknowledgements

This research project (AiF-FV-Nr. 11574 N / 1) has been sponsored by the Bundesministerium für Wirtschaft und Technologie (BMWi) via the Arbeitsgemeinschaft industrieller Forschungsvereinigungen "Otto von Guericke" e.V. (AiF). The support is gratefully acknowledged.

References

[1] **Drost, U., and Bölcs, A.:** Investigation of Detailed Film Cooling Effectiveness and Heat Transfer Distribution on a Gas Turbine Airfoil. *ASME-Paper,* no 98-GT-20, 1998

[2] **Eckert, E. R. G.:** Analysis of Film Cooling and Full-Coverage Film Cooling of Gas Turbine Blades. *ASME Journal of Engineering for Gas Turbines and Power,* vol. 106, pp. 206-213, 1984

[3] **Eriksen, V. L., and Goldstein, R. J.:** Heat Transfer and Film Cooling Following Injection through Inclined Circular tubes. *ASME Journal of Heat Transfer,* Vol. 16, pp. 239-245, 1974

[4] **Folayan, C. O., and Whitelaw, J. H.:** The Effectiveness of Two-Dimensional Film-Cooling Over Curved Surfaces. *ASME-Paper*, no 76-HT-31, 1976

[5] **Foster, N. W., and Lampard, D.:** The Flow and Film Cooling Effectiveness Following Injection Through a Row of Holes. *ASME Journal of Engineering for Power,* vol. 102, pp. 584-588, 1980

[6] **Goldstein, R. J., and Stone, L. D.:** Row-of-Holes Film Cooling of Curved Walls at Low Injection Angles. *ASME Journal of Turbomachinery,* vol. 119, pp. 574-579, 1997

[7] **Goldstein, R. J., Kornblum, Y., and Eckert, E. R. G.:** Film Cooling Effectiveness on a Turbine Blade. *Israel Journal of Technology,* vol. 20, no 4-5, pp. 193-200, 1982

[8] **Goldstein, R. J.:** Film Cooling. *Advances in Heat Transfer,* vol. 7, pp. 321-379, 1971

[9] **Haslinger, W., and Hennecke, D. K.:** The Ammonia and Diazo Technique With CO2-Calibration for Highly Resolving and Accurate Measurement of Adiabatic Film Cooling Effectiveness With Application to a Row of Holes. *ASME-Paper,* no 96-GT-438, 1996

[10] **Ito, S., Goldstein, R. J., and Eckert, E. R. G.:** Film Cooling of a Gas Turbine Blade. *ASME Journal of Engineering for Power,* vol. 100, pp. 476-481, 1978

[11] **Jabbari, M. Y., and Goldstein, R. J.:** Adiabatic Wall Temperature and Heat Transfer Downstream of Injection Through Two Rows of Holes. *ASME Journal of Engineering for Power,* vol. 100, pp. 303-307, 1978

[12] **Kruse, H.:** Effects of Hole Geometry, Wall Curvature and Pressure Gradient on Film Cooling Downstream of a Single Row. *AGARD Conference Proceedings,* no 390, pp. 1-13, 1985

[13] **Lander, R. D., Fish, R. W., and Suo, M.:** External Heat-Transfer Distribution on Film-Cooled Turbine Vanes. *Journal of Aircraft,* vol. 9, pp. 707-714, 1972

[14] **Lutum, E., von Wolfersdorf, J., Semmler, K., Dittmar, J., and Weigand, B.:** An Experimental Investigation of Film Cooling on a Convex Surface Subjected to Favourable Pressure Gradient. *submitted for Int. Journal of Heat and Mass Transfer,* 2001

[15] **Lutum, E., von Wolfersdorf, J., Weigand, B., and Semmler, K.:** Film Cooling on a Convex Surface: Part 1 Zero Pressure Gradient Flow. *International Journal of Heat and Mass Transfer,* no 43, pp. 2973-2987, 2000

[16] **Martinez-Botas, R. F., and Yuen, C. H. N.:** Measurement of Local Heat Transfer Coefficient and Film Cooling Effectiveness Through Discrete Holes. *ASME-Paper,* no 2000-GT-243, 2000

[17] **Mayle, R. E., Kopper, F. C., Blair, M. F., and Balley, D. A.:** Effect of Streamline Curvature on Film Cooling. *ASME Journal of Engineering for Power,* vol. 99, pp. 77-82, 1977

[18] **Nicolas, J., and Le Meur, A.:** Curvature Effects on a Turbine Blade Film Cooling. *ASME-Paper,* no 74-GT-156, 1974

[19] **Pedersen, D. R.:** Effect of Density Ratio on Film Cooling Effectiveness for Injection Through a Row of Holes and for a Porous Slot. *Ph.D. Thesis, University of Minnesota, USA,* 1972

[20] **Schwarz, S. G., and Goldstein, R. J.:** The Two-Dimensional Behaviour of Film Cooling Jets on Concave Surfaces. *ASME Journal of Turbomachinery,* vol. 111, pp. 124-129, 1989

[21] **Schwarz, S. G., Goldstein, R. J., and Eckert, E. R. G.:** The Influence of Curvature on Film Cooling Performance. *ASME Journal of Turbomachinery,* vol. 113, pp. 472-478, 1991

[22] **Sinha, A. K., Bogard, D. G., and Crawford, M. E.:** Gas Turbine Film Cooling: Flowfield Due to a Second Row of Holes. *ASME Journal of Turbomachinery,* Vol. 113, pp. 450-456, 1991

Paper Number: 6

Name of Discusser: P. Ireland, University of Oxford

Question:
Your measurement were made at unity coolant to free-stream density ratio. Could you comment on the effect that use of an engine representative density might have on the flow field?

Answer:
You are right, the measurements were made at a (unrealistic) density ratio of unity. One of the motivation for this study was, to create a data base for validations of CFD-calculations
Thus the density ratio of unity could be better.
I think the use of an engine-like density ratio leads to a reduced radius of the jet trajectory (see calculations of Ito 1978). Therefore you should have an increase of η on the convex and a decrease on the concave wall at same blowing rates)

Name of Discusser: W. B. de Wolf, National Aerospace Laboratory Emmeloord, NL,

Question:
Have you any data available on intermediate blowing rates and at what blowing rates do you expect lift-off of the orifice jets, depending on wall curvature?

Answer:
Yes, we have investigated blowing rates of 0,25 to 2 with steps of 0,25. For the configuration we used (blowing angle 40 °) I expect the jet lift off between 0,5 and 0,75 for all investigated curvature radii. I think the blowing rate, where the jets lift off differs a little bit depending on curvature radii, but in that mentioned small range.

Name of Discusser: B. Simon, MTU Aero Engines Munich

Question:
Are you planning to determine the htc additonally to the film cooling effectiveness?

Answer:
This was planned as a follow-up project.